IOPscience iopscience.iop.org

Home Search Collections Journals About Contact us My IOPscience

Dynamics of the ZnMgY icosahedral phase

This article has been downloaded from IOPscience. Please scroll down to see the full text article.

2002 J. Phys.: Condens. Matter 14 1847

(http://iopscience.iop.org/0953-8984/14/8/313)

View the table of contents for this issue, or go to the journal homepage for more

Download details:
IP Address: 171.66.16.27
The article was downloaded on 17/05/2010 at 06:12

Please note that terms and conditions apply.

INSTITUTE OF PHYSICS PUBLISHING JOURNAL OF PHYSICS: CONDENSED MATTER

J. Phys.: Condens. Matter **14** (2002) 1847–1863 PII: S0953-8984(02)30210-8

Dynamics of the ZnMgY icosahedral phase

K Shibata[1], R Currat[2], M de Boissieu[3], T J Sato[4], H Takakura[5] and A P Tsai[4]

[1]Institute for Material Research, Tohoku University, Sendai 980-77, Japan
[2]Institut Laue Langevin, BP 156, 38042 Grenoble, France
[3]Laboratoire de Thermodynamique et Physico-Chimie Metallurgiques, UMR CNRS 5614, INPG, ENSEEG, BP 75 38402, St Martin d'Heres Cedex, France
[4]Materials Engineering Laboratory, NIMS, 1-2-1, Sengen, Tsukuba 305-0047, Japan
[5]Advanced Materials Laboratory, NIMS, 1-1, Namiki, Tsukuba 305-0044, Japan

Received 30 October 2001, in final form 14 January 2002
Published 15 February 2002
Online at stacks.iop.org/JPhysCM/14/1847

Abstract

The dynamics of the icosahedral ZnMgY phase has been investigated on a single-grain quasicrystalline sample using inelastic neutron scattering. Similarly to other quasicrystals we observe well defined acoustic modes for values of the wavevector smaller than 0.3 Å^{-1}. We find a longitudinal sound velocity equal to 4800 m s^{-1} and an isotropic transverse sound velocity equal to 3100 m s^{-1}. The acoustic character and the broadening of transverse excitations has been studied extensively. We find that transverse excitations remain acoustic up to $q = 0.5$ Å^{-1}. For q lying between 0.3 and 0.5 Å^{-1} we observe a broadening, which is independent of the propagation or polarization direction, while the dispersion relation departs from linearity. For $q = 0.6$ Å^{-1} there is a resonance with an optic-like excitation located at about 10 meV and the signal can no longer be described by a single acoustic mode. For larger wavevectors we observe a broad distribution of modes, which can be split into three dispersionless optical bands located at 8, 12 and 17 meV. The 8 and 12 meV bands are associated with the crossing of pseudo-zone boundaries by the acoustic branch. A detailed comparison with results obtained in the i-AlPdMn phase shows significant differences: in particular the broadening of transverse acoustic modes is much less pronounced in the ZnMgY phase than in the i-AlPdMn one.

(Some figures in this article are in colour only in the electronic version)

1. Introduction

Quasicrystals are long-range ordered materials whose diffraction pattern presents symmetries incompatible with translational invariance. In a few systems they can be obtained as large single grains with a high degree of structural order, which allow detailed studies of their physical

 © 2002 IOP Publishing Ltd Printed in the UK

properties and of their collective dynamics to be performed. Indeed the quasiperiodic long-range order of the structure is believed to give rise to a specific dynamical response (see [1,2] for an introduction).

Theoretically, the study of the dynamics of quasicrystals is a complex problem. Analytical solutions have only been obtained in the one-dimensional case [3–16]. For two-dimensional and three-dimensional systems, results have been obtained by simulations on large-unit-cell periodic approximants [17–24], which contain the same building units as the quasicrystal. Because of the absence of periodicity the Bloch theorem breaks down. However quasicrystals, unlike amorphous systems, are highly ordered systems with well defined Bragg peaks. In the long-wavelength limit well defined acoustic modes exist and are measurable by inelastic neutron scattering close to the strong Bragg reflections: each strong Bragg reflection can thus be considered as a zone centre. Considering the quasiperiodic structure as a weak perturbation on a monatomic structure [25], the concept of the Brillouin zone can be extended to quasicrystals. First a generalized structure factor is computed, from which a series of special points, located around the origin of reciprocal space, are defined [26,27]: only those points which have a strong generalized structure factor are important. This set of points allows us to construct a series of pseudo-Brillouin zone boundaries (PZBs), which can be drawn around each strong Bragg reflection acting as a zone centre. In the perturbative approach, each time the acoustic branch crosses a PZB, there is a gap opening whose magnitude is proportional to the generalized structure factor: in other words the acoustic wave is Bragg reflected by the Fourier component of the atomic density associated with each special point in reciprocal space. The description of excitations in quasicrystals can thus be carried out in an extended zone scheme, where zone centres and PZBs are defined.

The nature of the eigenstates is also believed to be specific to quasicrystals. For the one-dimensional Fibonnacci chain, it has been shown that some modes are critical: they are neither extended as for a periodic crystal, nor localized with an exponential decay, as for disordered systems. Critical modes are localized on specific local environments, which are found infinitely many times in the quasiperiodic structure, and show a power law rather than an exponential decay. Similar properties have been observed in simulations on two-dimensional systems. For instance, some of the electronic eigenstates of large decagonal approximants present power law decay and are localized on specific local environments [28]. For three-dimensional systems, simulations of the vibrational properties on realistic models showed that there are 'confined' modes: in the case of Frank–Kasper-type quasicrystals, the eigenmodes are localized on highly frustrated sites at the intersection of disclination lines [22]. Such sites are quasiperiodically stacked in the structure. Because of the Conway theorem, which states that any local environment with a radius R can be found at least once in a sphere of radius $2R$, these environments are not independent and will 'feel' each other: this is what makes the major difference with localized modes in disordered systems.

Experimentally, dispersion relations have been measured by inelastic neutron scattering on single grains of the i-AlLiCu [29,30], i-AlCuFe [31,32], i-AlPdMn [33,34] and d-AlNiCo [35] phases. Comparisons with a periodic approximant have been carried out only for the AlLiCu system. The most detailed results were obtained for the icosahedral AlPdMn and decagonal AlNiCo phases for which large single grains of good structural quality have been obtained. In the icosahedral AlPdMn phase, well defined acoustic excitations are observed close to the strong Bragg reflections. For wavevectors smaller than 0.3 Å^{-1} they are resolution limited with an intensity scaling as expected for long-wavelength excitations in the acoustic regime. For larger wavevectors a rapid broadening of the acoustic excitations is observed, which corresponds to a mixing of the acoustic-like excitation with a series of broad (4 meV) dispersionless excitations located at 7, 12, 16 and 22 meV. The acoustic character of the

excitation is lost for wavevectors larger than 0.65 $Å^{-1}$. Although no gap could be detected at the crossing of the PZB, the low-energy optic modes have an energy corresponding to the crossing of the transverse acoustic branch with a PZB.

Decagonal phases have a structural anisotropy with a structure consisting of a stacking of quasiperiodic planes. We observed well defined acoustic excitations, presenting a broadening for transverse modes polarized in the periodic direction. For transverse modes polarized in the quasiperiodic plane a resonance splitting is observed at an energy transfer of 15 meV. This was interpreted as the result of the strong disorder present in the structure.

The ZnMgY icosahedral phase is particularly interesting for the study of dynamical properties: it can be obtained as large single grains with a good structural quality; its atomic structure is completely different from that of the i-AlPdMn phase. Although its detailed atomic structure has not yet been solved, the local order, and the atomic clusters constituting the i-ZnMgY phase, are believed to be different from those of the i-AlPdMn phase [36, 37]. In the i-AlPdMn phase the broadening of excitations in the acoustic regime begins for a wavelength of the order of 20 Å, which is of the same order of magnitude as the atomic cluster size. The study of the dynamics of the i-ZnMgY phase is thus of particular interest.

We present in this paper a complete study of the dynamics of the ZnMgY phase by inelastic neutron scattering on a single-grain sample. Section 2 gives the experimental details. An outline of the data analysis is given in section 3. The results of the measurements and analysis are given in section 4. First a detailed analysis of the transverse and longitudinal acoustic modes is given, followed by the presentation of the high-energy excitations in section 5. A discussion and conclusion are given in section 6.

2. Experimental details

A single grain of the ZnMgY phase has been prepared by the Bridgman technique. It was pulled at a 0.2 mm h^{-1} speed in a furnace with a temperature gradient equal to 6 K mm^{-1}, corresponding to a cooling rate of 1.2 K h^{-1} [38]. The composition of the single grain is $Zn_{60}Mg_{31}Y_9$. The sample was irregularly shaped with a volume equal to approximately $1 \times 0.9 \times 0.7$ cm^3.

The quasicrystalline and single-grain character of the sample was carefully checked by x-ray and neutron diffraction. Systematic reciprocal maps were recorded on a four-circle diffractometer mounted on a rotating anode Cu source. All Bragg spots could be indexed in the icosahedral $Fm35$ lattice. The intensity distribution of Bragg peak intensities was found to be very different to what is observed in the i-AlPdMn phase as illustrated in figure 1. In particular peaks with a high Q_{per} component are observed, as a result of the very different atomic structure of the ZnMgY icosahedral phase. A high-resolution x-ray diffraction pattern was carried out on the D2AM beam line [39]: unlike most of the i-ZnMgRE samples that were studied, Bragg peaks did not show any departure from their ideal position, confirming the icosahedral character of the phase. The width of the Bragg reflections showed a clear linear dependence on Q_{per} with a coefficient of proportionality equal to 0.005, to be compared with 0.0008 found in the best i-AlPdMn phases. The single-grain character of the bulk sample was finally checked by neutron diffraction. The sample mosaic was found to be equal to 0.1°, with a small companion grain one-tenth of the size located at 1° from the main one. Systematic scans carried out along the high-symmetry directions did not show any parasitic phase and could be indexed using a six-dimensional lattice parameter equal to 0.73 nm. Figure 2 presents a scan along a five-fold axis with some of the N/M indices given [40]. The high density of Bragg peaks makes the likelihood of multiple diffraction rather high, which sometimes leads to spurious signals in the inelastic scans.

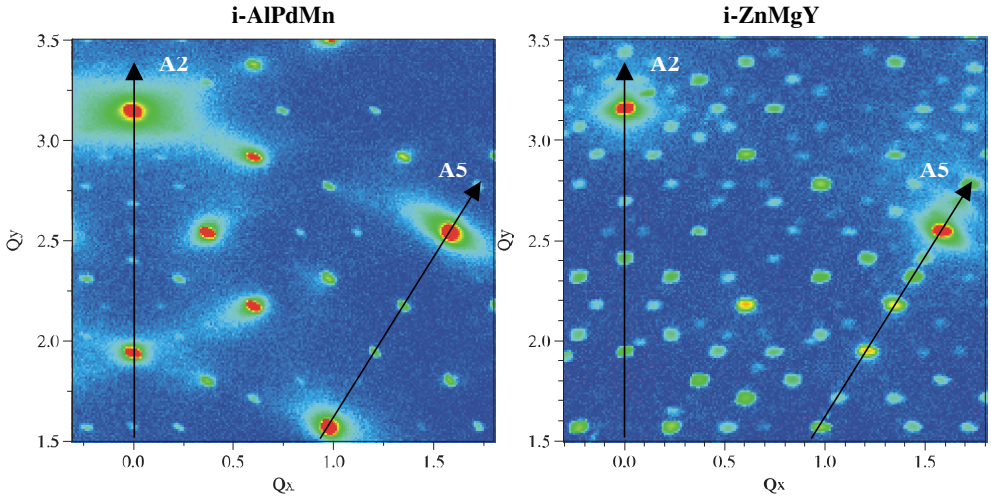

Figure 1. Systematic reciprocal space map recorded in the i-AlPdMn phase (left) and i-ZnMgY phase (right). Data were collected by using the Cu radiation of a rotating anode generator, in reflection geometry. The same area of reciprocal space is covered in both figures. To ease the comparison, Q_x and Q_y coordinates are given in $2\pi/a$ units. The Bragg peak intensity distribution is very different as the result of the very different atomic structures.

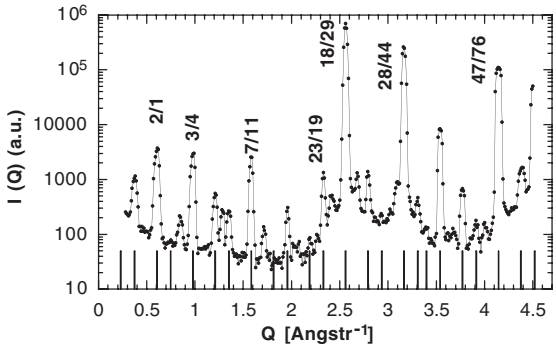

Figure 2. Longitudinal elastic Q-scan measured along a five-fold axis. All peaks can be indexed in the icosahedral quasilattice. Vertical lines show the theoretical position of Bragg peaks in the icosahedral lattice, with a Q_{per} cut-off set to 2.5 (in $2\pi/a$ units). Unindexed reflections correspond to higher Q_{per} reflections, to higher-order contamination or to multiple diffraction. A few N/M indices [40] are given.

Higher-energy excitations were measured on the IN8 three-axis spectrometer located on the thermal source of the ILL reactor. Scans were recorded with a fixed final wavevector equal to $k_f = 2.662$ Å^{-1}, using a vertically curved graphite monochromator, a 60′ collimation before the sample and a doubly curved graphite analyser. The energy resolution measured on a vanadium sample is equal to 1.1 meV. The energy resolution for dispersing modes depends on the slope of the dispersion relation, on the Q position and on the energy transfer. For transverse acoustic modes measured at $Q = 4.5$ Å^{-1} in the energy range 2–8 meV, the instrumental resolution is of the order of 1.3 meV. Longitudinal scans and some transverse scans were recorded with a flat analyser for better resolution: in this configuration the energy resolution is of the order of 1.7 meV for longitudinal acoustic phonons and 0.8 meV for transverse acoustic phonons.

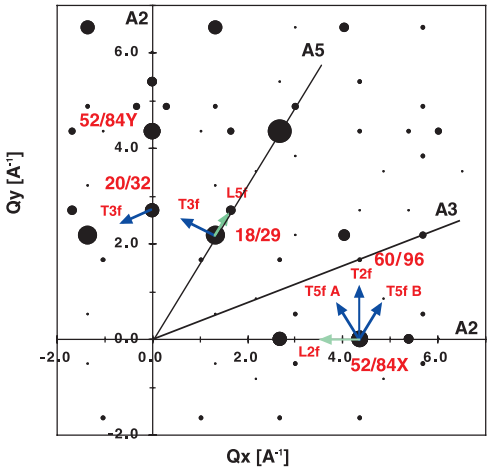

Figure 3. Twofold scattering plane. The size of the dots is proportional to the Bragg peak intensity. Bragg peaks around which measurements have been carried out are labelled with their N and M indices. Their corresponding six indices are given in table 1.

Table 1. Indices of a few Bragg reflections shown in figure 2. Q_{par} and Q_{per} are given in $2\pi/a$ units, where a is the six-dimensional lattice parameter equal to 0.73 nm.

N	M	M_{ul}	h/h'	k/k'	l/l'	Q_{par}	Q_{per}
18	29	12	1/2	2/3	0/0	2.995	0.17
20	32	30	2/4	0/0	0/0	3.15	0.28
52	84X	30	4/6	0/0	0/0	5.096	0.18
52	84Y	30	0/0	4/6	0/0	5.096	0.18
60	96	20	2/2	4/6	0/0	5.455	0.49

Low-energy excitations were measured on the HER three-axis spectrometer located on the curved guide facing the cold source of the JRR-3M reactor in JAERI. Scans were recorded with a fixed initial wavevector $k_i = 1.545$ Å^{-1}, using a vertically curved graphite monochromator, a cold Be filter before the sample and a flat graphite analyser. The collimations were open–40′–40′–40′ for the longitudinal acoustic mode measurements and open–40′–80′–80′ for the transverse acoustic mode measurements with vanadium resolution widths of 0.12 and 0.22 meV respectively. For transverse acoustic modes measured at $Q = 2.5$ Å^{-1} in the energy range around 2 meV, the resolution is of the order of 0.8 meV. For longitudinal acoustic modes measured at $Q = 2.5$ Å^{-1} in the energy range around 1.6 meV, the resolution is of the order of 0.7 meV, i.e. half the size of that for the IN8 measurements.

All measurements were carried out in the two-fold scattering plane for which the Bragg pea k intensity distribution is shown in figure 3. The main reflections around which excitations have been measured are labelled with their N and M indices, as proposed by Cahn *et al* [40], in figure 3. The corresponding six-dimensional indices are given in table 1.

3. Data analysis

As explained in the introduction, the definition of a zone centre and thus of the $\boldsymbol{q}$ wavevector of an excitation is in principle not possible for quasicrystals. It is only in the acoustic regime that a direct correspondence between the measured spectra and phonon excitations can be

made accurately. In the following we choose as zone centre the strongest Bragg reflections. Around each of these zone centres there is a hierarchy of PZBs, defined as $\boldsymbol{G} + \boldsymbol{q}_{ZB}$ where $\boldsymbol{G}$ is the reciprocal lattice vector of the zone centre, and $2\boldsymbol{q}_{ZB}$ is a vector of the reciprocal quasilattice. In a simple perturbation approach, there is a gap opening each time the acoustic branch crosses such a zone boundary, and the slope of the dispersion relation vanishes at this point. The magnitude of the gap is proportional to the generalized structure factor so that only PZBs associated with a large generalized structure factor are meaningful. However, since a structural model is not yet available, it is not possible to compute the mass-weighted structure factor as was done for the i-AlPdMn phase. Nevertheless, we shall define the important PZBs according to the measured structure factor. Starting from the origin, the strongest structure factors are found along a three-, five- and two-fold axis, with Q values equal to 0.89, 0.97 and 1.03 Å^{-1}. The first pseudo-Brillouin zone boundary is thus obtained by the intersection between an icosahedron, a dodecahedron and a triacontahedron. This volume has a shape very close to a sphere of radius 0.48 Å^{-1}. The next PZB is obtained as the intersection of a dodecahedron and a triacontahedron τ times larger than the previous one (where τ is the golden mean). Around each strong Bragg reflection there is thus a stacking of these two main PZBs. They can actually be viewed as the midpoints between the strong Bragg reflections observed in figures 2 and 3. From this simple approach we can thus expect a gap opening in the dispersion curve at $q = 0.48$ Å^{-1}.

A phonon can strictly be defined only in the long-wavelength limit or acoustic regime. In this case a clear selection rule exists, which allows the measurement of the phonon dispersion relation. The response function of an acoustic mode measured at a reciprocal space position $\boldsymbol{Q} = \boldsymbol{G} + \boldsymbol{q}$, where $\boldsymbol{G}$ is the reciprocal vector of the Bragg reflection chosen as zone centre, and F_{el} its structure factor, reads

$$S(\boldsymbol{Q}, E) = \frac{\langle n(E) + \frac{1}{2} \pm \frac{1}{2} \rangle}{E_{T(L)}(\boldsymbol{q})} (\boldsymbol{e}_{T(L)} \cdot \boldsymbol{Q})^2 F_{el}^2(Q) \delta(E \pm E_{T(L)}). \tag{1}$$

This relation can be used to assess the acoustic character of a given phonon branch: as long as the acoustic character holds, the normalized intensity of the measured excitation I_{norm}, as defined in expression (2) below, should be constant.

$$I_{norm(T,L)} = I_{ph(T,L)} \cdot E^2 \tag{2}$$

where $I_{ph(T,L)}$ is obtained by integrating (1) over energies.

For larger wavevectors the situation is much more complex: a simple question such as 'what is the wavevector of the excitation?' cannot be answered. The only quantity which is measured is the response function $S(\boldsymbol{Q}, E)$. Nevertheless, in the following, results will be displayed as pseudo-dispersion relations in an extended zone scheme, with the vector $\boldsymbol{q}$ defined with reference to the strong Bragg reflections.

The energy, width and intensity of the different observed excitations were extracted by fitting the $S(\boldsymbol{Q}, E)$ function with a superposition of damped harmonic oscillators (DHOs) when in the acoustic regime and by a superposition of Gaussians for high-energy excitations. For each experimental configuration the instrumental broadening has been taken into account [41]. The reported widths thus correspond to intrinsic values. The smallest detectable excitation width is of the order of 0.1 meV.

4. Acoustic regime

4.1. Transverse modes

Transverse modes propagating along a direction parallel to two-, three- and five-fold directions were measured around several reflections lying on a two- or five-fold symmetry axis (see figure 3). As expected for icosahedral symmetry we found that the transverse sound velocity is independent of the direction of propagation and polarization, with a value equal to 3100 ± 100 m s^{-1} in good agreement with ultrasonic measurements [42].

Examples of constant-q energy scans, with $\boldsymbol{q}$ parallel to a three-fold axis, measured around the 18/29 reflection are shown in figure 4. The left panel corresponds to measurements carried out on the HER spectrometer. Thanks to the good energy resolution low q TA phonons could be measured. Excitation profiles are well defined and the observed line widths correspond to the calculated instrumental resolution for q smaller than 0.3 Å^{-1} as shown by the solid curve in figure 4. The right-hand panel corresponds to measurements carried out on the IN8 spectrometer. The dispersion relation deduced from these measurements is shown in figure 5. A study of the normalized intensity shows that below $q = 0.5$ Å^{-1} the modes have a clear acoustic character, with a normalized intensity that is constant. As will be shown in section 5, above 0.5 Å^{-1} the measured signal is the superposition of the acoustic signal and of dispersionless excitations: in that regime it is difficult to give a precise value for the width of the measured TA phonons.

It is thus only for q between 0 and 0.5 Å^{-1} that a precise study of TA mode broadening could be carried out. Above $q = 0.3$ Å^{-1} TA phonons present a significant broadening, to reach a width of the order of 1 meV at $q = 0.5$ Å^{-1}. Above $q = 0.2$ Å^{-1} we also observe that the dispersion relation departs from a linear behaviour with a downward curvature.

The broadening of phonons may originate from many physical processes, but roughly two main hypotheses can be formulated: it can be due to the finite lifetime of TA acoustic phonons because of interactions of the phonons with defects or it can be the superposition of several modes, because the selection rule does not apply perfectly (i.e. because the wavevector q is not a good quantum number). In the classical limit the interaction of acoustic phonons with defects should lead to the response function of a DHO, with a width growing as q^2. The DHO response function has a characteristic Lorentzian-like shape. If the observed broadening is the result of the superposition of several modes we might expect a more Gaussian shape for the response function. To try to distinguish between these two possibilities some measurements were made with a flat analyser around the two-fold 52/84 reflection: with this configuration the instrumental phonon line width is equal to 0.8 meV. The broadening is already visible for $q = 0.3$ Å^{-1}. The response function is slightly better fitted with a DHO function than with a Gaussian one, but a clear distinction is difficult to make. The q range for which we observe a broadening of the TA acoustic phonons, unmixed with other contributions, is limited to $q = 0.3$, 0.4 and 0.5 Å^{-1}. Within experimental accuracy the broadening seems to be more rapid than q^2.

In this q range we could not detect any anisotropy of the broadening, for TA acoustic modes propagating along the two-, three- and five-fold directions. Note that the more precise results were obtained for two-fold TA modes measured around the 52/84 reflection because the signal is much larger in this area due to the Q^2 factor in the phonon intensity (see expression (1)).

All these results thus suggest that below $q = 0.5$ Å^{-1} a single acoustic phonon is observed and that the broadening observed is due to the phonon interaction with defects. It is interesting to calculate the mean free path of the acoustic phonon at the border of the acoustic regime. For a wavevector $q = 0.5$ Å^{-1}, corresponding to a wavelength of 1.3 nm, TA phonons have

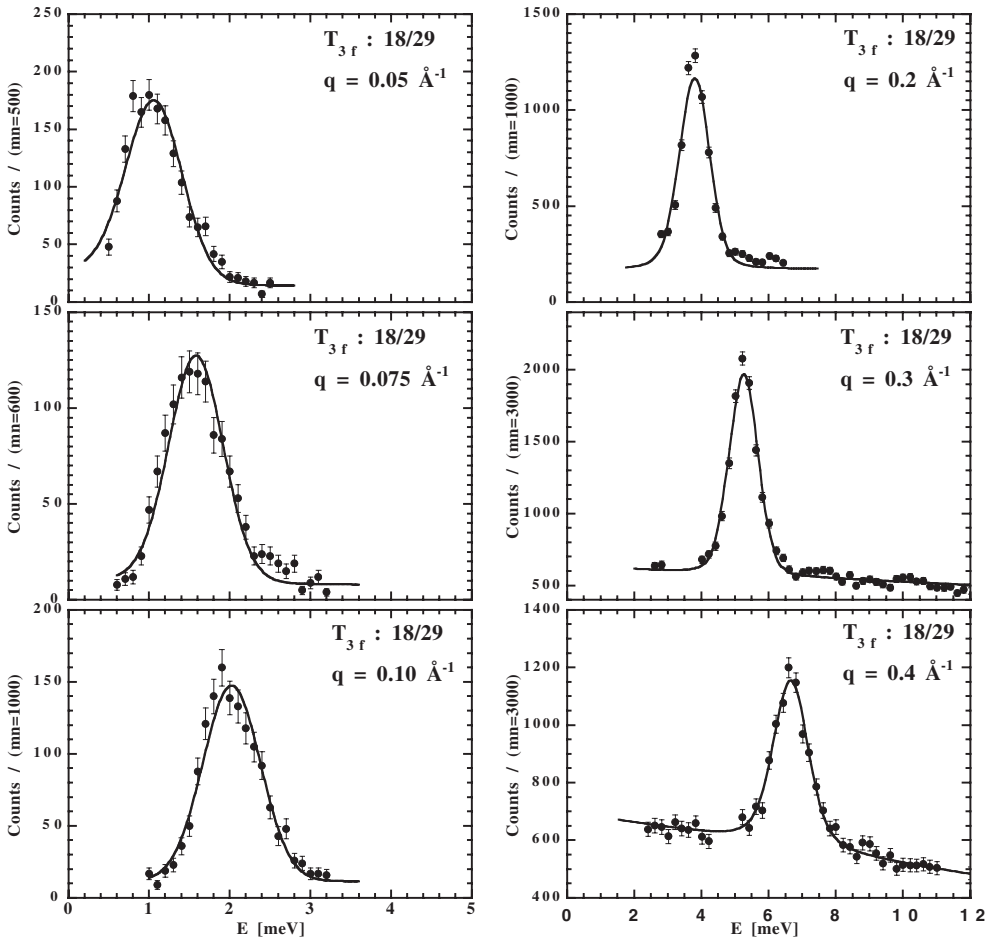

Figure 4. TA phonons propagating along the three-fold direction measured near the 18/29 reflection. Left panel: measurements carried out on the HER spectrometer (cold source of the JAERI reactor). Right panel: measurements carried out on the IN8 spectrometer. The solid curve is a fit to the data using a DHO convoluted with the instrumental resolution. Note the scale range change between the left and the right-hand panel. For q smaller than or equal to 0.3 Å^{-1} the observed curve profile is exactly that of the resolution function of the instrument.

an energy of 8 meV, and the group velocity deduced from the dispersion relation is equal to 1800 m s^{-1}. Their lifetime is equal to 1.3×10^{-12} s, corresponding to a mean free path equal to 2.3 nm.

Finally, as already observed for the i-AlPdMn phase, no gap opening could be detected when the acoustic branch crosses the first main PZB, shown as a vertical dashed line in figure 5. This means that the gap, if any, has a width smaller than 0.2 meV.

4.2. Longitudinal modes

Longitudinal acoustic modes propagating along a two- and a five-fold direction have been measured using a flat analyser in order to limit the resolution broadening.

At small q well defined excitations are measured as shown in figure 6 for LA phonons propagating along a five-fold direction. The top two panels ($q = 0.03$ and 0.05 Å^{-1})

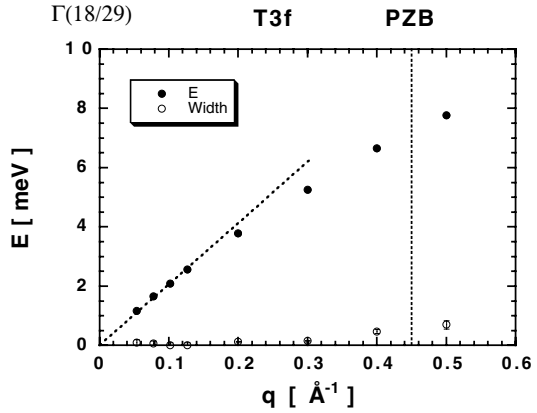

Figure 5. Dispersion relation of TA phonons propagating along a three-fold axis corresponding to the measurements of figure 3. Closed and open symbols represent the position and width of the excitations respectively. The main PZB is shown as a vertical dashed line.

correspond to measurements carried out on the HER spectrometer and the bottom four to measurements carried out on IN8. As usual for longitudinal modes with a steep slope a transverse acoustic mode contribution is also visible on low-q spectra as a result of the finite vertical divergence of the neutron beam. This contribution has been either subtracted or fitted as shown for $q = 0.05$ Å^{-1}. The corresponding dispersion curve is reported in figure 7. We find a longitudinal sound velocity equal to 4800 ± 150 m s^{-1}, in good agreement with ultrasonic measurements shown as a dashed line. Above $q = 0.2$ Å^{-1} the dispersion curve slightly departs from a linear dispersion and the width of the excitations shows a marked increase. Because of the low signals, LA modes could not be measured for q larger than 0.4 Å^{-1}. In this q range, the width of LA modes increases as q^2, as has already been observed in the decagonal phase. The normalized intensity remains constant up to $q = 0.4$ Å^{-1}, which demonstrates that the signal remains acoustic up to about 11 meV. At this point the phonon wavelength is 1.6 nm and its group velocity is 3300 m s^{-1}. The phonon lifetime is 0.8×10^{-12} s, corresponding to a mean free path of 2.7 nm, i.e. of the same order as for transverse acoustic phonons.

5. High-energy excitations

The most detailed analysis of acoustic phonon broadening and high-energy excitations has been carried out along an axis parallel to the Y two-fold axis, starting from the Bragg point with indices 52/84X (see figure 3; to distinguish reflections lying on the X and Y two-fold axes, we label them with their N/M indices and the X or Y label). In this configuration, the selection rule allows us to measure transverse acoustic phonons propagating along a two-fold direction and polarized along an orthogonal two-fold direction. We measured carefully both the width and the intensity of the excitations. As already said in section 4, for small q there is a single excitation whose width is resolution limited. For q larger than 0.2 Å^{-1} acoustic excitations present a marked broadening, and the dispersion relation departs from linearity. Up to $q = 0.5$ Å^{-1} the normalized intensity remains constant, which demonstrates that the mode has an acoustic character up to this value. For $q = 0.6$ Å^{-1} there is an abrupt change in the normalized intensity, which increases by a factor almost equal to two. This is illustrated in figure 8, where the acoustic contribution has been calculated from lower-energy scans and is

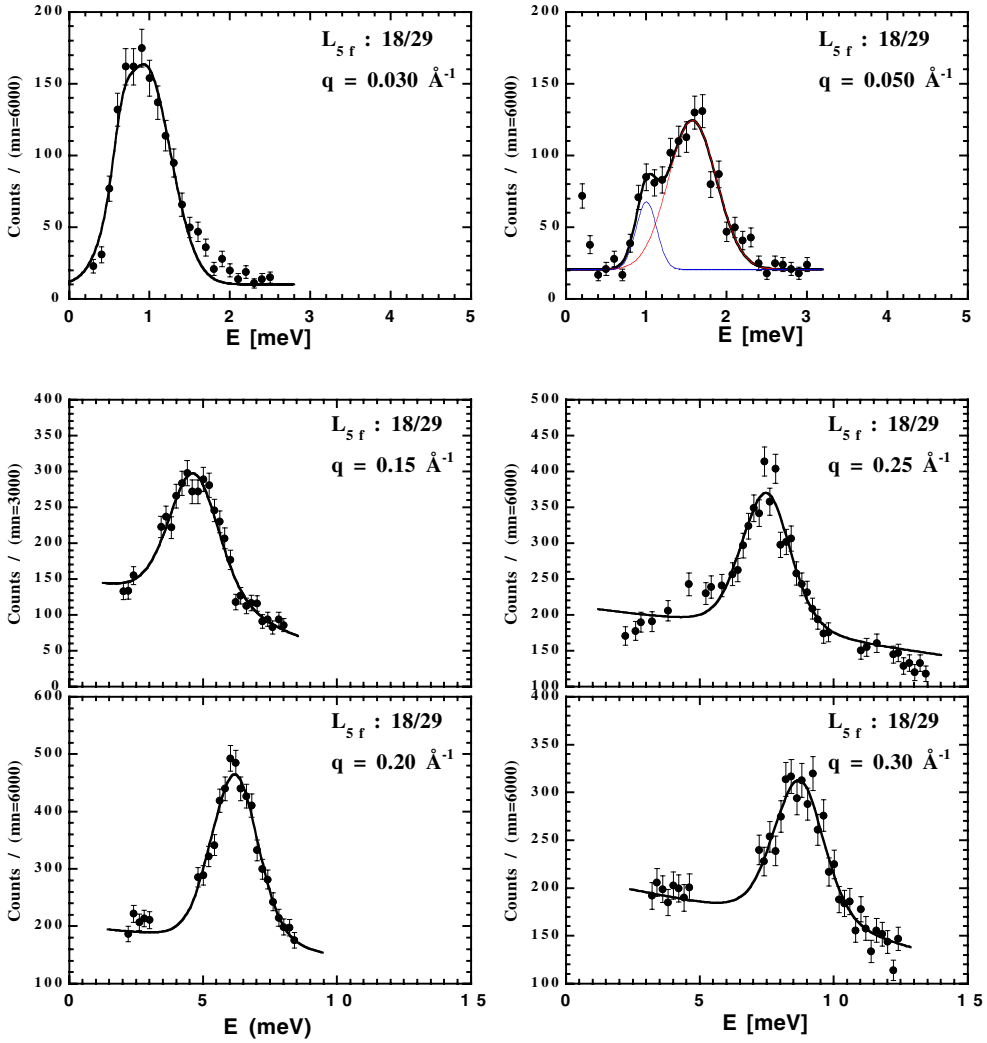

Figure 6. Constant-energy scans for LA phonons propagating along a five-fold direction and measured near the 18/29 reflection. The top two panels and bottom four panels correspond to measurements carried out on the HER spectrometer and IN8 respectively.

shown as a solid curve: the measured signal is clearly broader than the acoustic contribution and can only be reproduced assuming at least two overlapping contributions.

The complete set of measured spectra is shown in figure 9. Above $q = 0.6$ Å^{-1} there is a mixing of several excitations but fitting the observed signal with two excitations is difficult because the two contributions overlap and give rise to a single broad peak. From $q = 0.9$ Å^{-1} at least three contributions located at 8, 12 and 16 meV are necessary to reproduce the data. The 8 meV signal contains the TA contribution of an out-of-plane reflection which shows some small dispersion and an intensity maximum for $q = 1.1$ Å^{-1} (figure 9, bottom right-hand panel) corresponding to a minimum distance between the measuring plane and the out-of-plane reflection. Beside this TA out-of-plane contribution, the 8 meV signal also contains a dispersionless optic-like contribution as will be shown in the following. The existence of three

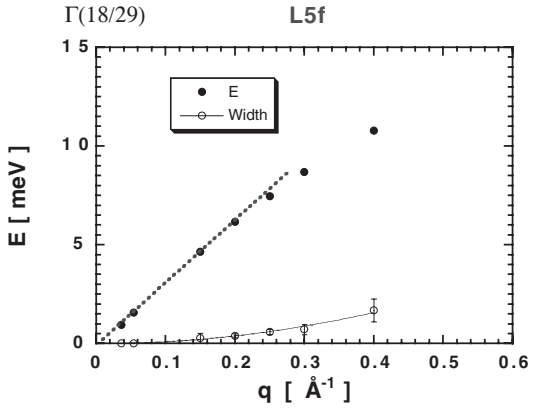

Figure 7. Dispersion relation for LA modes measured in figure 5. Open symbols refer to the width of the excitations.

dispersionless bands (8, 12 and 16 meV) is further confirmed by measurements of transverse excitations carried out around the reflection 52/84 Y located on the Q_y two-fold axis. Again, for high-q wavevectors, the signal is the superposition of two modes at around 11 and 16 meV, plus another excitation at 8 meV, which in this case does not contain an out-of-plane contribution, since no strong reflection is located close enough to this reciprocal space area.

Finally this high-energy study has been completed by a measure at the Q point with reciprocal coordinates in Å^{-1} (2.5, 2.5, 0). This point is far away from any strong Bragg reflection in or out the scattering plane: the closest strong reflection is the five-fold 18/29 reflection, located at a relative q value of 1.2 Å^{-1}. A study of the response function at this point is thus free from any acoustic contamination. The measured signal is shown in figure 11. At least three excitations can be observed, which are centred at $E = 8$, 12 and 16 meV: this confirms the presence of an optic-like mode with an energy of 8 meV. The three optic modes are thus observed in various regions of reciprocal space and present a negligible dispersion. Each of these modes is however very broad with a full width at half maximum equal to 4 or 5 meV.

The dispersion relation corresponding to excitations measured between the Γ points 52/84X and 60/96 is reported in figure 10. The four different observed excitations are labelled accordingly in the figure: one transverse two-fold acoustic mode (full circle), and three optic-like modes located at 8 meV (diamonds), 12 meV (squares) and 17 meV (triangles). The 8 meV mode is the superposition of an out-of-plane acoustic-like mode and an optic-like mode. As explained above, this 8 meV mode has been observed in regions of reciprocal space where no acoustic contribution could be accounted for, which justifies labelling as an optic mode on the dispersion curve. The width of the acoustic mode is indicated by an open circle, and grows rapidly above $q = 0.2$ Å^{-1}. Since the high-energy signal is very broad, a precise determination of the width of the optic-like excitations is rather difficult and is not reported in the figure. Measurements have been carried out up to $q = 1.4$ Å^{-1} from the Γ point 52/84X, which is located at 0.27 Å^{-1} from the point 60/96: the acoustic contribution from this medium-intensity reflection could thus be measured and is reported as a full circle in the figure. As a guideline, the linear acoustic dispersions originating from the two Γ points are shown as dashed lines. As was observed for transverse modes propagating in the three-fold direction, no anomaly is observed when the acoustic branch crosses the main PZB, indicated as a vertical dashed line.

The strong coupling between the TA acoustic mode and the 8 meV excitation which occurs at $q = 0.6$ Å^{-1} has been checked for transverse acoustic phonons propagating along a five-

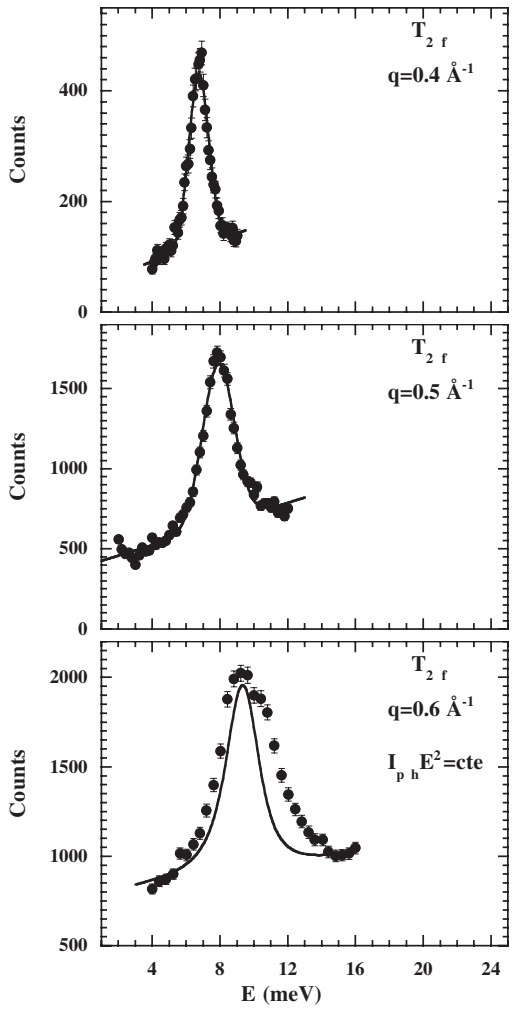

Figure 8. Transverse excitations propagating along a two-fold direction measured around the reflection 52/84X located along the two-fold X axis. The solid curve is a fit of the excitation using a DHO model and a constant normalized intensity (see text). At $q = 0.6$ Å^{-1} an acoustic model clearly failed to reproduce the data and at least two contributions have to be considered.

fold axis and measured close to the Bragg point 52/84X (arrows labelled T5fA and T5fB in figure 3). Due to the limited range in measured q wavevectors the signal has been fitted by a single excitation reported as a full circle in figure 12. As for TA phonons propagating along a two-fold axis, both the width and the normalized intensity present an anomaly when q goes from 0.5 to 0.6, which shows that this coupling does not depend on the propagation direction of the TA phonon.

6. Discussion and conclusion

The observed response function can be divided into two regions: the acoustic regime, visible experimentally close to strong Bragg peaks, and an optic-like regime where several excitations are mixed. The crossover between the two regimes is very sharp and occurs for a wavevector

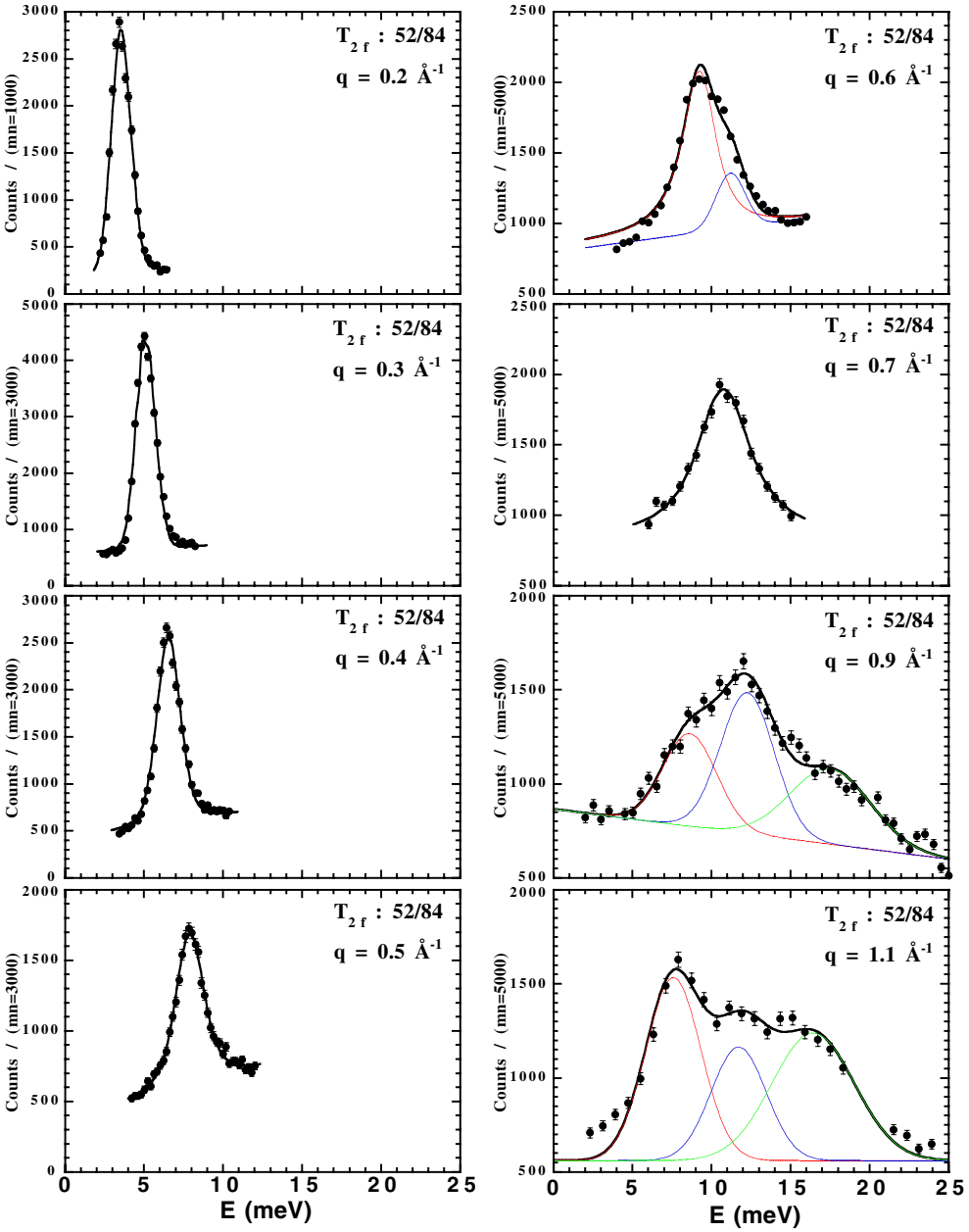

Figure 9. Transverse excitations propagating along a two-fold direction measured around the reflection 52/84X from $q = 0.2$ to 1.1 Å^{-1}. For q larger than 0.5 Å^{-1} several excitations are mixed and the signal is reproduced by the superposition of two or three Gaussian contributions, each one with a width of the order of 4 meV. Individual contributions are shown as thin solid curves for $q = 0.9$ and 1.1 Å^{-1}.

equal to $q = 0.5$ and 0.4 Å^{-1} for TA and LA modes respectively. Expressed in term of the phonon energy the TA and LA regime holds for phonons having an energy smaller than 8 and 11 meV respectively.

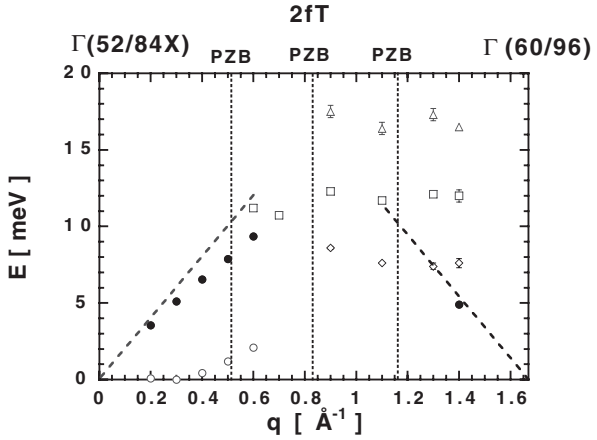

Figure 10. Dispersion curve for excitations measured between the Bragg points 52/84*X* and 60/96. Some of the corresponding measurements are shown in figures 7 and 8. The acoustic contribution is shown by a full solid circle and its width by an open one. Optic-like excitations located at an energy of 8, 12 and 16 meV are shown by open diamonds, squares and triangles respectively. The acoustic sound velocity, as deduced from low-q measurement, is shown as a dashed line starting from the two Γ points. The main PZBs are indicated by vertical dashed lines.

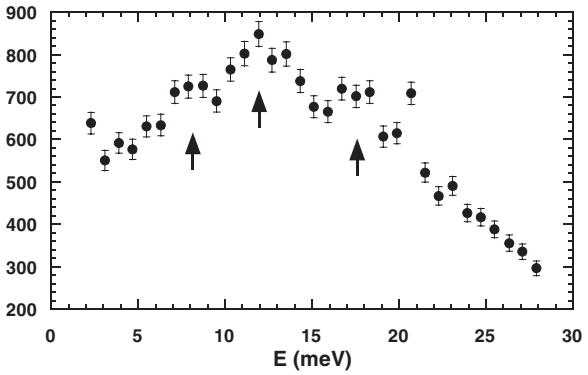

Figure 11. Signal measured at the Q point with coordinates (2.5, 2.5, 0). This reciprocal point is located far away from any strong Bragg peak to be free from an acoustic-like contribution. The signal is very broad and contains at least three contributions located at 8, 12 and 17 meV shown by arrows.

Both TA and LA excitations are resolution limited for q smaller than 0.3 Å^{-1}. For larger wavevector the LA phonon width grows as q^2, as expected for phonon attenuation by defects, whereas the width of TA modes growths faster. The broadening is independent of the phonon propagation direction or polarization. The acoustic regime is characterized by a normalized inelastic intensity which is constant up to $q = 0.5$ Å^{-1}. At the boundary of the acoustic regime LA and TA phonons have a wavelength of 1.2 nm and a mean free path of the order of 2.5 nm. This small mean free path justifies setting a limit to the single-phonon regime at about 0.5 Å^{-1}: the observed mean free path corresponds to only twice the wavelength. It would be meaningless to label single-propagative-phonon, higher-energy excitations which are broad and would thus have a mean free path smaller than their corresponding wavelength.

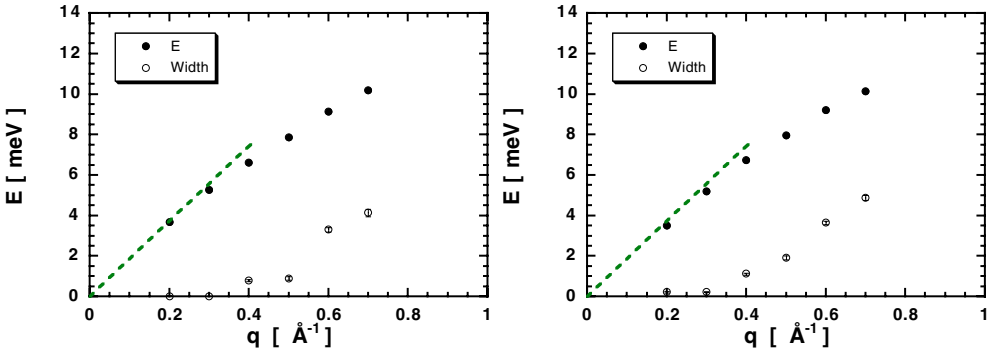

Figure 12. Dispersion relation for TA acoustic modes propagating along a five-fold axis and measured around the 52/84X Bragg reflection. Full and open circles represent the position and the width of the TA phonon respectively. Left- and right-hand panels correspond to T5fA and T5fB respectively, as shown in figure 3.

The first important PZB is found for $q = 0.5$ Å^{-1} along the two-fold axis. A this point we expect the slope of the dispersion curve to vanish and the opening of a gap. Although the acoustic phonon was sharply defined, we could not detect any sign of a gap opening or any other anomaly. It is only for $q = 0.6$ Å^{-1} that an anomaly in the phonon intensity is observed. At this point the observed response function corresponds to the superposition of at least two contributions and there is a strong coupling between the acoustic mode and an optic-like mode with an energy of about 10 meV. Such a coupling had not been observed previously for icosahedral phases. We suggest that this coupling is the signature of the crossover between two regimes.

Above this value the response function is a mixture of several modes. Although the signal is extremely broad at least three optic branches can be defined: they are located at $E = 8$, 12 and 16 meV respectively. Two of these bands (12 and 16 meV) have been observed in the generalized vibrational density of states (GVDOS) measured by Suck [43] on a powder sample. The lower one at $E = 8$ meV is not seen in the GVDOS, where the signal is still in the ω^2 regime. This might be because the acoustic contribution still dominates the GVDOS signal at this energy. However, the response function measured on a powder sample does show the same flat band at 8 meV [43].

Although no gap opening is observed at the crossing of the PZB, we can note that the energy at which the TA branch crosses the PZB is about 8 meV, i.e. the same as the lowest-energy optic-like mode. In fact, if we artificially continued the TA branch above $q = 0.5$ Å^{-1}, it would cut the second main PZB at an energy of 12 meV. We can thus associate the two low-energy optic excitations with the crossing of the PZB, similarly to what has been observed in the i-AlPdMn phase. Such an interpretation is consistent with theoretical calculations on an i-AlZnMg [22] whose diffraction pattern presents similarities with that of the i-ZnMgY one. The calculated dynamical structure factor, using a realistic pair potential, shows stationary modes at the PZB which extend as dispersionless excitations away from the PZB similarly to that observed.

When these results are compared with what has been obtained in other quasicrystalline phases significant differences are observed. A strong coupling between an acoustic and an optic excitation has also been observed in the decagonal AlNiCo phase, for transverse acoustic phonons polarized in the quasiperiodic plane. However, in this case the signal could be clearly separated into two contributions, in contrast to the present case. Moreover the coupling was attributed to the large amount of structural disorder present in the d-AlNiCo phase, whereas the i-ZnMgY phase is much more ordered.

A detailed comparison between the i-AlPdMn and i-ZnMgY excitation spectra is more relevant. The sound velocities in i-ZnMgY are about 20% smaller than in the i-AlPdMn phase. However, because of the differences in the six-dimensional lattice parameter the acoustic branches cross the PZB at about the same energies in both phases, leading to dispersionless branches at the same energies. For q smaller than 0.5 Å^{-1} the broadening of the excitation is much more rapid in the i-AlPdMn phase than in i-ZnMgY: for instance at $q = 0.5$ Å^{-1} the transverse acoustic phonon has a width equal to 2.5 meV in the i-AlPdMn phase to be compared with 1.3 meV for i-ZnMgY. On the other hand, at $q = 0.6$ Å^{-1} we found a strong intensity anomaly in the i-ZnMgY phase not seen in i-AlPdMn. In other words the 12 meV optic-like mode in the ZnMgY phase couples more strongly with the transverse acoustic branch than in the i-AlPdMn phase. Thus detailed comparison shows that there are significant differences between the response function of the two systems. This is certainly to be related to the large difference in the atomic structure of both phases.

Finally it is interesting to connect the length-scales at the observed acoustic crossover to the atomic structure of the i-ZnMgY phase. The diameter of the icosahedral clusters usually considered in the description of icosahedral Frank–Kasper phases is of the order of $D_{cl} = 1.2$ nm. There is a quasiperiodic packing of these clusters with a mean inter-cluster distance, which is also of the order of D_{cl}. The crossover between the acoustic and the optic regime occurs for phonons having a wavelength of the order of D_{cl} and a mean free path of the order of $2D_{cl}$. It was suggested by Janot [44] that the hierarchical structure and the cluster distribution in quasicrystals plays a major role in the phonon spectrum: phonon wavefunctions would be strongly localized on clusters whose smaller size is of the order of D_{cl}. Because of the quasiperiodic long-range order, the phonon wavefunctions would decay exponentially between two equivalent sites $2D_{cl}$ apart, leading to a strong damping of phonons. The crossover we find in this experiment is fairly consistent with this picture: in other words at $q = 0.5$ Å^{-1} the phonon wave can still feel the quasiperiodic order, although it is strongly damped by its interaction with localized modes. This situation is different from amorphous systems (see for instance [45]), where long-range order does not exist: although local environments similar to what is found in the corresponding quasicrystal might exist in the amorphous state, the strong structural disorder leads to a localization of the states in the high-energy region and to a very restricted acoustic region. At the other extreme a simple periodic packing will not give rise to a strong damping. We thus suggest that both the damping and the strong coupling between a TA mode and a localized state observed in the present experiment are characteristic of the quasiperiodic order.

In conclusion we observe two distinct regimes in the excitation spectrum of the i-ZnMgY phase: an acoustic one for q smaller than 0.5 Å^{-1} and an optic-like regime above. We find a longitudinal sound velocity equal to 4800 m s^{-1} and an isotropic transverse sound velocity equal to 3100 m s^{-1}. The acoustic character and the broadening of transverse excitations has been studied extensively. We find that transverse excitations remain acoustic up to $q = 0.5$ Å^{-1}. For q lying between 0.3 and 0.5 Å^{-1} we observe a broadening, which is independent of the propagation or polarization direction, while the dispersion relation departs from linearity. This broadening is significantly smaller than what was previously observed in the i-AlPdMn phase. For $q = 0.6$ Å^{-1} there is a resonance with an optic-like excitation located at about 10 meV and the signal can no longer be described by a single acoustic mode. For larger wavevectors we observe a broad distribution of modes, which can be split into three dispersionless optical bands located at 8, 12 and 17 meV. The 8 and 12 meV bands are associated with the crossing of PZBs by the acoustic branch. The crossover between the two regimes is abrupt and occurs for TA phonons with a wavelength of the order D_{cl}, where D_{cl} is the diameter of the building atomic clusters, and a mean free path equal to $2D_{cl}$. We suggest that this behaviour is characteristic of the quasicrystalline state.

Acknowledgment

We thank E Kats for fruitful discussions.

References

[1] Quilichini M and Janssen T 1997 *Rev. Mod. Phys.* **69** 277
[2] Janot C 1992 *Quasicrystals: a Primer* (Oxford: Oxford Science)
[3] De Lange C and Janssen T 1981 *J. Phys. C: Solid State Phys.* **14** 5269
[4] Ashraff J A and Stinchcombe R B 1989 *Phys. Rev.* B **39** 2670
[5] Ostlund S, Pandit R, Rand D, Schellenhuber H J and Siggia E D 1983 *Phys. Rev. Lett.* **50** 1873
[6] Kohmoto M, Kadanoff L P and Tang C 1983 *Phys. Rev. Lett.* **50** 1870
[7] Ostlund S and Pandit R 1984 *Phys. Rev.* B **29** 1394
[8] Luck J M and Petritis D 1986 *J. Stat. Phys.* **42** 289
[9] Lu J P, Odagaki T and Birman J 1986 *Phys. Rev.* B **33** 4809
[10] Tamura S and Wolfe J P 1987 *Phys. Rev.* B **36** 3491
[11] Kohmoto M, Sutherland B and Tang C 1987 *Phys. Rev.* B **35** 1020
[12] Lu J P and Birman J 1987 *Phys. Rev.* B **36** 4471
[13] Lu J P and Birman J 1987 *Phys. Rev.* B **38** 8067
[14] Janssen T and Kohomoto M 1988 *Phys. Rev.* B **38** 5811
[15] Levitov L S 1989 *J. Physique* **50** 707
[16] Benoit C, Poussigue G and Azougarh A 1990 *J. Phys.: Condens. Matter* **2** 2519
[17] Patel H and Sherrington D 1989 *Phys. Rev.* B **40** 11 185
[18] Los J and Janssen T 1990 *J. Phys.: Condens. Matter* **2** 9553
[19] Los J, Janssen T and Gahler F 1993 *J. Physique* I **3** 1431
[20] Hafner J and Krajci M 1993 *Europhys. Lett.* **21** 31
[21] Hafner J and Krajci M 1993 *Phys. Rev.* B **47** 1084
[22] Hafner J and Krajci M 1993 *J. Phys.: Condens. Matter* **5** 2489
[23] Hafner J and Krajci M 1999 *Physical Properties of Quasicrystals* ed Z M Stadnik (New York: Springer) p 209
[24] Poussigue G, Benoit C, de Boissieu M and Currat R 1994 *J. Phys.: Condens. Matter* **6** 659
[25] Smith A P and Ashcroft N W 1987 *Phys. Rev. Lett.* **59** 1365
[26] Niizeki K 1989 *J. Phys. A: Math. Gen.* **22** 4295
[27] Niizeki K and Akamatsu T 1990 *J. Phys.: Condens. Matter* **2** 2759
[28] Fujiwara T, Mitsui T and Yamamoto S 1996 *Phys. Rev.* B **53** 2910
[29] Goldman A I, Stassis C, Bellissent R, Mouden H, Pyka N and Gayle F W 1991 *Phys. Rev.* B **43** 8763 (short communication)
[30] Goldman A I, Stassis C, Deboissieu M, Currat R, Janot C, Bellissent R, Moudden H and Gayle F W 1992 *Phys. Rev.* B **45** 10 280
[31] Quilichini M, Heger G, Hennion B, Lefebvre S and Quivy A 1990 *J. Physique* **51** 1785
[32] Quilichini M, Hennion B, Heger G, Lefebvre S and Quivy A 1992 *J. Physique II* **2** 125
[33] de Boissieu M, Boudard M, Bellissent R, Quilichini M, Hennion B, Currat R, Goldman A I and Janot C 1993 *J. Phys.: Condens. Matter* **5** 4945
[34] Boudard M, de Boissieu M, Kycia S, Goldman A I, Hennion B, Bellissent R, Quilichini M, Currat R and Janot C 1995 *J. Phys.: Condens. Matter* **7** 7299
[35] Dugain F, de Boissieu M, Shibata K, Currat R, Sato T J, Kortan A R, Suck J-B, Hradil K, Frey F and Tsai A P 1999 *Eur. Phys. J.* B **7** 513
[36] Yamamoto A, Weber S, Sato A, Kato K, Ohshima K, Tsai A P, Nikura A, Hiraga K, Inoue A and Masumoto T 1996 *Phil. Mag. Lett.* **73** 247
[37] Takakura H, Shiono M, Sato T J, Yamamoto A and Tsai A P 2001 *Phys. Rev. Lett.* **86** 236
[38] Sato T J, Takakura H and Tsai A P 1998 *Japan. J. Appl. Phys.* **37** 663
[39] Letoublon A *et al* 2000 *Mater. Sci. Eng.* **294–6** 127
[40] Cahn J W, Shechtman D and Gratias D 1986 *J. Mater. Res.* **1** 13
[41] Bouvet A, Filhol A and Kulda J 1997 Pkfit software manual *ILL Report* 97BO03T
[42] Sterzel R *et al* 2001 *Mater. Res. Soc. Symp. Proc.* **643** K1.4.1
[43] Rouijaa M, Suck J-B and Sterzel R 2001 *J. Alloy Compounds* at press
[44] Janot C 1996 *Phys. Rev.* B **53** 181
[45] Suck J-B, Rudin H, Gunterhodt H-J and Beck H 1981 *J. Phys. C: Solid State Phys.* **14** 2305